scientific reports



OPEN

Investigations on whether imagesharpening algorithm can improve the determination of severity of diabetic retinopathy in ultrawidefield fundus photographs

Jun Takeuchi^{1,2}, Hiromi Ohara¹, Tadashi Yokoi¹, Takashi Koto¹ & Makoto Inoue^{1⊠}

The purpose of this study was to determine the effectiveness of image-sharpening algorithms in detecting the severity of diabetic retinopathy (DR) in ultra-widefield (UWF) fundus photographs. This was a retrospective observational study of 100 UWF fundus photographs of 100 diabetic patients. The Optos UWF photographs of eyes with DR were enhanced using medical image enhancement software, and 3 masked retinal specialists evaluated the severity of DR according to the International Clinical Diabetic Retinopathy (ICDR) Disease Severity Scale. This scale is a five-stage classification system for DR. The skewness and kurtosis were measured to assess the image contrast. The results showed that the severity of the DR in the original and enhanced images did not agree in 14 of the 100 eyes. Eleven eyes were classified to have more severe retinopathy in the enhanced images than in the regular images. Twenty intraretinal retinal hemorrhages were detected in each of the four quadrants, definite venous beading in two quadrants, and prominent intraretinal microvascular abnormalities. These lesions were detected significantly more often in the enhanced images (P = 0.03). The skewness and kurtosis were significantly improved in the enhanced images (P < 0.001, P < 0.001, respectively). We conclude that the image-sharpening algorithms can improve the detection of lesions in the Optos UWF images, and improve the accuracy of the severity index in DR. These improvements make the imagesharpening algorithm a valuable tool for assessing the severity of DR.

Keywords Image-sharpening algorithm, Diagnosis, Diabetic retinopathy, Severity scale

The rising global prevalence of diabetes has resulted in a concomitant increase in the incidence of diabetic retinopathy (DR), a microvascular complication of diabetes mellitus^{1–3}. Accurate assessments of the severity of the DR, and the selection of an appropriate treatment are crucial in preventing visual impairments caused by this vision-threatening disorder⁴.

There are several classification systems for evaluating the severity of DR including the International Clinical Diabetic Retinopathy (ICDR) Disease Severity Scale⁵. This standard classification is based on color fundus photographs, and recent studies have highlighted the benefits of using ultra-widefield (UWF) fundus photographs for this. A UWF fundus photograph covers 80% of the total retina in a single image⁶⁻⁹. However, several technical shortcomings have been identified in the Optos UWF images including that they were pseudocolor images that differed from the actual ophthalmoscopic color images. There is also a reduction in the resolution of the far temporal and nasal peripheral retina, distortions of the peripheral retina, and the presence of artifacts caused by the eyelashes^{10,11}. Consequently, even among retina specialists, there are instances when the assessments of the severity of DR using UWF images do not correspond to those determined by conventional fundus photographs^{5,12}.

New techniques have been tried to improve medical images using image sharpening algorithms that are not arbitrary. These algorithms have been used to assess radiographic and magnetic resonance images^{13–15}, and photographs of the fundus of the eye in ophthalmology^{16–19}. Tasaki and associates¹⁹ have reported that image processing can remove honeycombs which are multiple cystic airspaces with thick walls that are clustered

¹Kyorin Eye Center, Kyorin University School of Medicine, 6-20-2 Shinkawa, Mitaka-shi, Tokyo, Japan. ²Department of Ophthalmology, Nagoya University Graduate School of Medicine, Nagoya, Japan. [⊠]email: inoue-eye@ks.kyorin-u.ac.jp

together and resembles a honeycomb. Honeycombs indicate significant tissue damage, and their removal by image-sharpening algorithms has led to a marked enhancement of their visibility in the surgical field during 27-gauge endoscopic vitrectomy. Our research team has demonstrated that image-sharpening algorithms can improve the clarity of the surgical field during 3D heads-up surgery^{17,18}. This was achieved by a reduction of the skewness and kurtosis of the light distribution of the objects of interest.

In ophthalmology, image-sharpening algorithms have been used mainly during ophthalmic surgeries^{17–19}. However, these algorithms can also be applied to the examination of the images of the retina such as in UWF photographs. However, as best we know, image-sharpening algorithms have not been used to determine the severity of DR.

Thus, the purpose of this study was to determine whether medical image enhancement software will improve the classification on the severity of DR. To accomplish this, the original UWF fundus photographs and their image-enhanced photographs of 100 eyes of 100 patients with DR were assessed. The examiners were three masked retinal specialists, and the images were assessed in accordance with the ICDR Disease Severity Scale.

Materials and methods

Ethics statement

The procedures used in this study conformed to the tenets of the Declaration of Helsinki, and they were approved by the Institutional Review Board of Kyorin University School of Medicine (2023-2261).

Patients who met the inclusion criteria received a detailed explanation of the ophthalmic procedures including the use of a medical image enhancer, and all signed an informed consent form. All the patients consented to our review of their medical images and their anonymized use in medical publications.

Participants and clinical measurements

This was a retrospective observational study that examined the UWF fundus photographs of 100 eyes of 100 patients with a history of diabetes and were patients of the Ophthalmology Department at Kyorin University Hospital. The fundus of 100 eyes were photographed with the Optos UWF scanning laser ophthalmoscope (California, Optos Inc, Dunfermline, UK) under mydriasis, and the images were then processed using a medical image enhancement software (Soft-MIEr*, Logic & Design, Tokyo, Japan). This algorithm optimizes the contrast and restores the resolution of the images by narrowing the point-spread function which differs from typical image processing methods that adjust the dynamic range of the contrast ^{16,19}. Additionally, the color tone was adjusted by calculating the brightness ratio for each pixel and processing it to create more natural colors. This algorithm contained several adjustable parameters, and the following settings were used. For contrast correction, the intensity correction was set at 70%, the contrast intensity was set at 5, and the calculation unit was set at 100. For color tone correction, the intensity was set at 320 and the dynamic range correction was set at 0. For the dark area compensation, the blur radius was set at 0.5, dark area compensation was set at 10%, compensation threshold was set at 50%, and the balance of dark area compensation and contrast correction was set at 50%.

One hundred UWF images that had not undergone any image processing and the same 100 UWF images that had undergone image processing were compared as the "original image group" and the "enhanced image group". Fifty-six of the 100 eyes also underwent wide-field optical coherence tomography angiography (OCTA) in a 12 mm x 12 mm scan with Plex Elite (Carl Zeiss Meditec, Dublin, California, USA) or a 12 mm x 15 mm scan with Xephilio (OCT-S1, Canon Inc., Tokyo, Japan) to confirm the results of the UWF images. OCTA was used to detect vascular lesions such as intraretinal microvascular abnormalities (IRMAs) and retinal neovascularizations and to confirm the results when IRMAs were detected in the UWF images. OCTA was also used to confirm the accuracy of results retrospectively when the severity of DR on UWF images differed between the two groups.

The severity of the DR for each image was determined by three masked retinal specialists in accordance with the ICDR Disease Severity Scale. The presence or absence of the three signs of severe non-proliferative diabetic retinopathy (NPDR) was also evaluated in the same manner, namely, the presence of 20 intraretinal hemorrhages in each of the four quadrants, definite venous beading in two quadrants, and prominent IRMAs in 1+quadrants. All evaluators used the same screen with the same brightness. Evaluators were only allowed to enlarge the image and were not allowed to edit the image, such as altering the contrast. If the results of the three differed, the severity of the disease agreed upon by any two was used as the final evaluation result.

Skewness and kurtosis

The skewness and kurtosis were used as indicators of the image contrast and were measured with the ImageJ fiji software²⁰. Skewness is a measure of the asymmetry of the image and indicates the degree to which the distribution of pixels is concentrated on one side of the peak intensity. When the absolute value of the skewness is near zero, the image is balanced and not excessively dark or bright²¹.

The kurtosis of an image is a measure of the sharpness and height of the central peak in the histogram of the brightness of the pixels. If the kurtosis is high, there are a significant number of pixels with the same pixel value in the image, indicating a lack of contrast²¹.

Statistical analyses

All statistical analyses were performed using the SPSS software (ver. 29.0.2.0; IBM Corp., Armonk, NY, USA). For comparisons between the two groups, Wilcoxon signed-rank test was used depending on the result of the Shapiro–Wilk test. Chi-Square (χ^2) Tests of Independence and χ^2 goodness-of-fit test were used to analyze the contingency tables. Data are presented as the mean \pm standard deviation. Statistical significance was set at P < 0.05.

Age years (mean ± SD)	64.2±13.3
Male/female (eyes)	73/27
Left/right (eyes)	51/49
BCVA logMAR units (mean ± SD)	0.13 ± 0.30
Phakic/Pseudophakic (eyes)	81/19

Table 1. Baseline characteristics. SD, standard deviation; BCVA, best-corrected visual acuity.

Enhanced image group							
			No apparent retinopathy	NPDR			-
	(eyes)		Mild	Moderate	severe	PDR
		ent	26				l
	Ž	apparent retinopathy	26	2			
dn	П	PliM		5	6		
Original image group		Mi		3	6		
	NPDR	Moderate		1	41	3	
	\\\\\\\\\\\\\\\\\\\\\\\\\\\\\\\\\\\\\	Mo					
		severe			2	9	
	Ш		 			115	
		PDR					5
			l		<u> </u>		

NPDR, non-proliferative diabetic retinopathy; PDR, proliferative diabetic retinopathy

Fig. 1. Comparisons of the severity of diabetic retinopathy in original and image enhanced ultra-widefield fundus photographs. Comparisons of the severity of diabetic retinopathy between the original and enhanced image groups based on the International Clinical Diabetic Retinopathy Disease Severity Scale. The severity of diabetic retinopathy of the original and enhanced images was not the same in 14 of the 100 eyes. Three eyes had more severe retinopathy in the original image group, and 11 eyes had more severe retinopathy in the enhanced image group (P = 0.03, χ^2 goodness-of-fit test). NPDR, non-proliferative diabetic retinopathy; PDR, proliferative diabetic retinopathy.

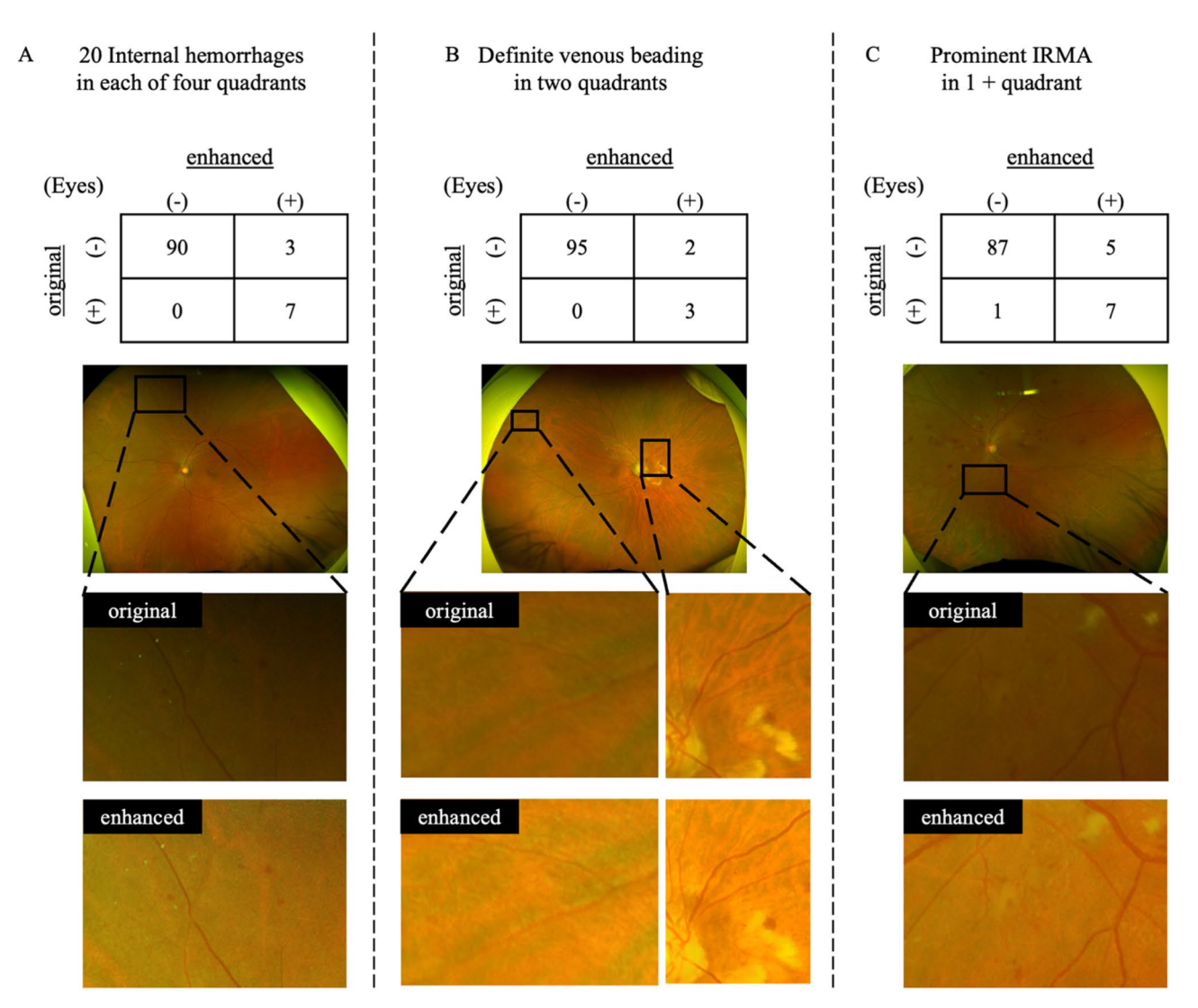
Results

The demographics of the 100 eyes of 100 patients at the baseline are summarized in Table 1. The mean age was 62.2 ± 13.3 years with a range from 28 to 88 years. The mean BCVA was 0.13 ± 0.30 logMAR units with a range from -0.08 to 1.70 logMAR units. There were 73 male patients with 51 left and 49 right eyes. There were 81 eyes that were phakic and 19 eyes with pseudophakia; 51 of the 81 eyes with phakia had been diagnosed with cataracts.

Three evaluators determined the severity of DR according to the ICDR Disease Severity Scale in the original and enhanced image groups. Inter-rater agreement was assessed by intraclass correlation coefficient (ICC). The results were ICC=0.84 (95% confidence interval: 0.78–0.88) for the original image group and ICC=0.81 (95% confidence interval: 0.74–0.86) for the enhanced image group, indicating very high inter-rater agreements (P<0.001 and P<0.001, respectively).

The severity of DR was compared between the original photographs and the enhanced photographs. Eighty-six (86%) of the 100 eyes had the same severity score of DR between the two sets of photographs. Fourteen eyes (14%) had a significant difference in the severity score (Fig. 1). Of these 14 eyes, 11 eyes were classified with greater severity in the enhanced image group, and 3 eyes had greater severity in the original image group. In these 14 inconsistent eyes, the enhanced image group had significantly higher rate of severe retinopathy (P=0.03, χ^2 goodness-of-fit test). Six of the 14 eyes also underwent OCTA, and when the UWF and OCTA images were re-examined, the more severe determination was accurate in all six eyes.

The incidence of each of the three signs of NPDR was compared between the two groups of photographs. For "the presence of 20 intraretinal hemorrhages in each of the four quadrants", 7 eyes in the original image group and 10 eyes in the enhanced image group were classified as having these findings (Fig. 2A). If we assume that there are no false positives due to the nature of the evaluation methods, then the sensitivity of the original image group is 70%, while that of the enhanced image group is 100%. Similarly, the finding of "definite venous beading in two quadrants" was observed in 3 eyes in the original image group and 5 eyes in the enhanced image



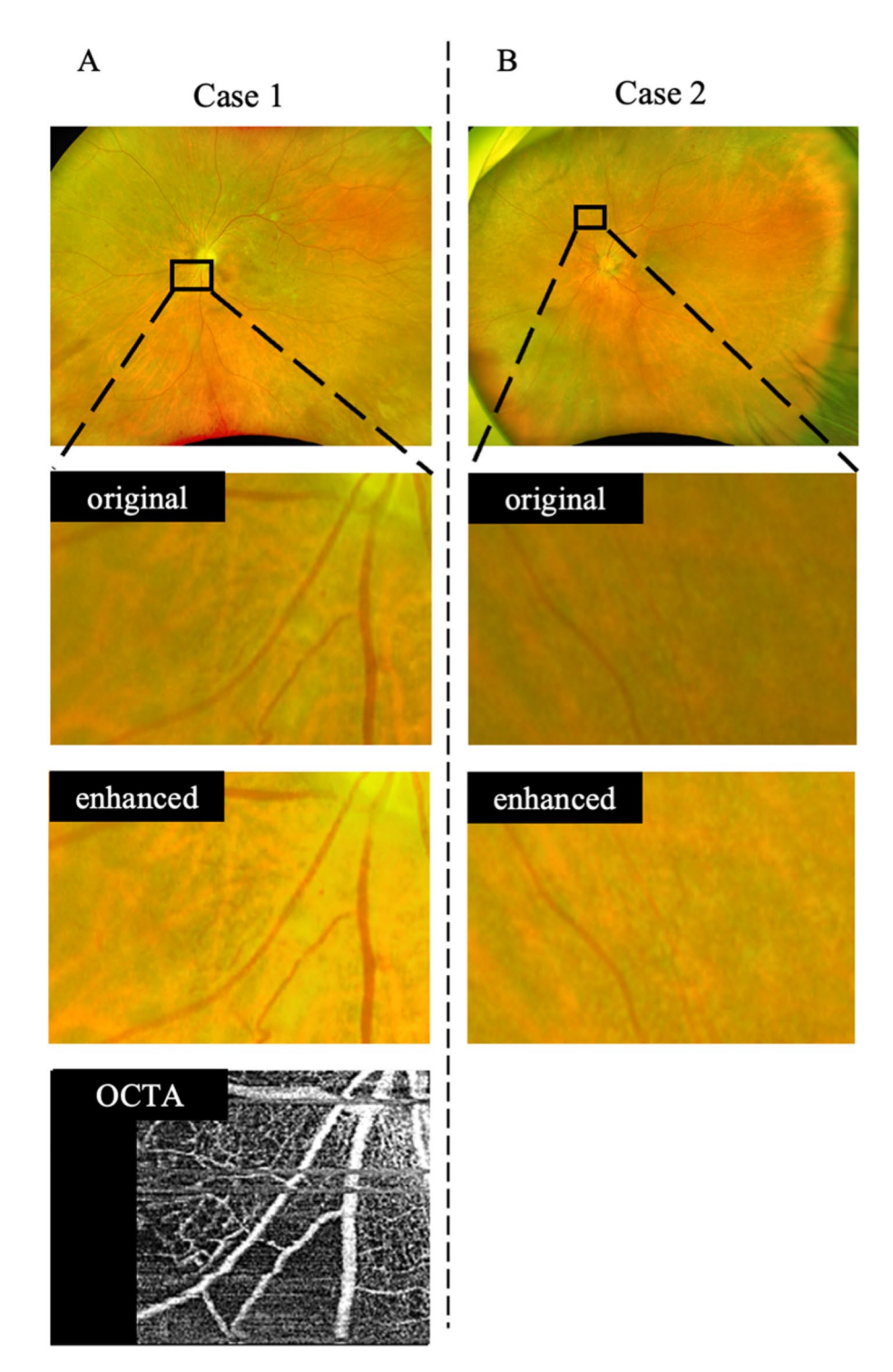
IRMA, intraretinal microvascular abnormalities

Fig. 2. Presence of severe NPDR findings. The diagnostic criteria for severe NPDR were: **(A)** Twenty intraretinal hemorrhages in each of the four quadrants: **(B)** Definite venous beading in two quadrants. **(C)** Prominent intraretinal microvascular abnormalities (IRMA) in 1 + quadrant cross tables and fundus photographs of representative cases. The detection sensitivity for any lesion in the enhanced image is high, and the image is bright and clear in the periphery as well as in the center of the image. NPDR, non-proliferative diabetic retinopathy.

group (Fig. 2B), with a sensitivity of 60% and 100%, respectively. The finding of prominent IRMAs or abnormal blood vessels in the retina in 1+quadrant was observed in 8 eyes in the original image group and 12 eyes in the enhanced image group (Fig. 2C). This represents sensitivities of 62% and 92% respectively. OCTA was performed in 12 of the 13 eyes determined to have IRMAs in at least one of the two groups, and IRMAs were also detected in all of the 12 eyes by OCTA.

In the 3 eyes of the original image group that had a greater severity, one eye had the difference in the presence of 20 intraretinal hemorrhages in each of the four quadrants, and the two eyes had that in the prominent IRMAs or abnormal blood vessels in the retina in 1+quadrant (Fig. 3). The presence of 20 intraretinal hemorrhages in the four quadrants of the fundus may be unstable when the number of intraretinal hemorrhages was around 20. As for the presence of IRMAs, the image processing enhanced the weak IRMAs and reduced the difference from normal retinal vessels, which may have blurred the judgment of whether it was IRMA or normal intraretinal vessels. However, the final result was still IRMA due to the winding path of the vessels compared to normal intraretinal vessels in both the UWF and OCTA images (Fig. 3). Of the 11 eyes with severe disease in the enhanced image group, three eyes had differences in the three findings of severe NPDR, but two of these eyes also had differences in IRMA determination.

To evaluate the contrast of the images, the skewness and kurtosis of the images of the two groups were calculated. The mean skewness decreased significantly from 1.57 ± 0.49 in the original image group to 0.67 ± 0.28



OCTA, optical coherence tomography angiography

Fig. 3. Two cases with intraretinal microvascular abnormalities in which the severity of diabetic retinopathy in the original image was greater than the enhanced image. Comparing the original and enhanced images for intraretinal microvascular abnormalities (IRMAs), the image processing enhanced the weak IRMAs and reduced the difference from normal retinal vessels. This processing may have affected the judgment of whether it was an IRMA or normal intraretinal vessels. The final result was that IRMA due to the meandering vessels compared to normal intraretinal vessels in both the ultra-widefield fundus photographs (**A**, **B**) and optical coherence tomography angiography images (A). OCTA, optical coherence tomography angiography.

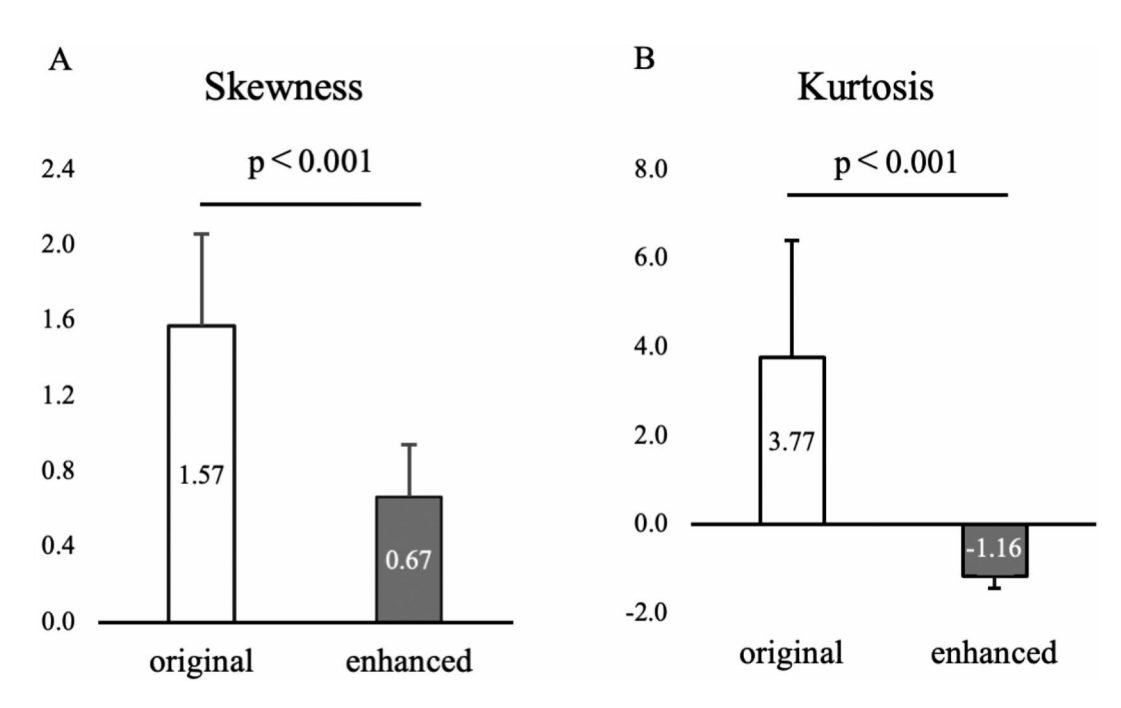


Fig. 4. Comparison of skewness and kurtosis. Comparisons of the skewness (**A**) and kurtosis (**B**) between original and enhanced image sets of photographs, Wilcoxon signed-rank sum test.

in the enhanced image group (P<0.001, Fig. 4A). The mean kurtosis decreased significantly, from 3.77 ± 2.63 in the original image group to -1.16 ± 0.24 in the enhanced image group (P<0.001, Fig. 4B).

Discussion

The findings indicate that medical image enhancement software improved the detection of lesions leading to a higher severity index in eyes with DR. The ICDR Disease Severity Scale is composed of five levels with severe NPDR and proliferative diabetic retinopathy (PDR) having a high risk of vision loss. In addition, it has also been shown that 50% of the severe NPDR eyes will progress to PDR within 1 year and 71% within 3 years⁵. The results shown in Fig. 1 show that there was no significant difference in the grading of the PDR between the original image group and the enhanced image group. However, there were differences in the grading between mild and moderate NPDR and between moderate and severe NPDR. These differences have the potential of influencing clinical decisions.

The clinical significance of these results is that in DR, which necessitates long-term management, the imagesharpening algorithm increased the ability to identify early signs of a severe disease and offers the possibility of prompt interventions.

Our team has reported that the same algorithms were able to process live images in real-time, thereby enhancing intraoperative visibility during 3D heads-up surgery^{17,18}. In the image processing that adjusts the dynamic range of the contrast, the color information is typically not modified, and only the brightness information is altered^{22,23}. Consequently, image processing may occasionally result in images that appear monochromatic with inadequate chromatic adjustments. The proprietary image-sharpening algorithm used in this study enhanced the image quality by optimizing contrast and restoring the resolution of the images through the narrowing of the point-spread function^{16,19}. In this image-sharpening algorithm, the color tone is calculated from the ratio of brightness change for each pixel unit and subsequently processed to create natural colors for the entire image as a parameter of color adjustment by regulating the coefficient at the time of the calculations. Thus, this calculation-based enhancement is different from the images produced by artificial intelligence.

The UWF images used have a weakness of being darker in the periphery than in the center of the image. It is possible that the algorithm provides appropriate contrast and color adjustments for each area of the image from the center to the periphery, and this may be the reason for the improved detection of lesions. From this point of view, the algorithm has advantages in detecting lesions in the periphery of the retina in UWF images and may be useful in detecting lesions in the peripheral retina such as retinal tears.

A limitation of this study was the absence of accurate data for a comparative analysis of the severity of the DR including actual fundus examinations by ophthalmologists between the two groups. In other words, the algorithm was found to enhance the identification of lesions and determine more severe DR. However, it did not directly demonstrate whether it was more accurate. However, a subsequent re-examination of the UWF and OCTA images in which only one group exhibited the lesion revealed that all images had the same findings, and no false positives were identified. Therefore, the findings that the algorithm produced a more accurate determination is valid.

In conclusion, the application of image-sharpening algorithms with appropriate contrast and color adjustment facilitates the detection of DR lesions, thereby enhancing the accuracy of the severity index of DR. We conclude

that the image enhancement software is a valuable tool for an accurate assessment of the severity of DR using UWF images.

Data availability

The datasets analyzed and generated during the current study are available from the corresponding author upon reasonable request.

Received: 29 January 2025; Accepted: 26 February 2025

Published online: 02 April 2025

References

- Teo, Z. L. et al. Global prevalence of diabetic retinopathy and projection of burden through 2045: Systematic review and Metaanalysis. Ophthalmology 128, 1580–1591 (2021).
- 2. Widyaputri, F., Rogers, S. & Lim, L. Global estimates of diabetic retinopathy prevalence and progression in pregnant individuals with preexisting diabetes: A meta-analysis. *JAMA Ophthalmol.* 40, 1137–1138 (2022).
- 3. Cioana, M. et al. Global prevalence of diabetic retinopathy in pediatric type 2 diabetes: A systematic review and meta-analysis. *IAMA Netw. Open.* 6, e231887 (2023).
- 4. Grading diabetic retinopathy. From stereoscopic color fundus photographs—an extension of the modified airlie house classification. ETDRS report number 10. Early treatment diabetic retinopathy study research group. *Ophthalmology* **98**, 786–806 (1991).
- Wilkinson, C. P. et al. Proposed international clinical diabetic retinopathy and diabetic macular edema disease severity scales. Ophthalmology 110, 1677–1682 (2003).
- 6. Liu, S. L. et al. A randomised trial of non-mydriatic ultra-wide field retinal imaging versus usual care to screen for diabetic eye disease: Rationale and protocol for the Clearsight trial. *BMJ Open.* 7, e015382 (2017).
- 7. Silva, P. S. et al. Peripheral lesions identified by mydriatic ultrawide field imaging: Distribution and potential impact on diabetic retinopathy severity. *Ophthalmology* **120**, 2587–2595 (2013).
- 8. Talks, S. J., Manjunath, V., Steel, D. H., Peto, T. & Taylor, R. New vessels detected on wide-field imaging compared to two-field and seven-field imaging: Implications for diabetic retinopathy screening image analysis. *Br. J. Ophthalmol.* **99**, 1606–1609 (2015).
- 9. Wessel, M. M. et al. Ultra-wide-field angiography improves the detection and classification of diabetic retinopathy. *Retina* 32, 785–791 (2012).
- Hirano, T. et al. Assessment of diabetic retinopathy using two ultra-wide-field fundus imaging systems, the Clarus and optos
 systems. BMC Ophthalmol. 18, 332 (2018).
- Spaide, R. F. Peripheral areas of nonperfusion in treated central retinal vein occlusion as imaged by wide-field fluorescein angiography. Retina 31, 829–837 (2011).
- 12. Srinivasan, S. et al. Inter-observer agreement in grading severity of diabetic retinopathy in wide-field fundus photographs. *Eye* (Lond). 37, 1231–1235 (2023).
- 13. Clark, J. L., Wadhwani, C. P., Abramovitch, K., Rice, D. D. & Kattadiyil, M. T. Effect of image sharpening on radiographic image quality. *J. Prosthet. Dent.* 120, 927–933 (2018).
- 14. Tsuboyama, T. et al. Impact of deep learning reconstruction combined with a sharpening filter on Single-Shot fast Spin-Echo T2-Weighted magnetic resonance imaging of the uterus. *Invest. Radiol.* 57, 379–386 (2022).
- 15. Yeoh, H. et al. Deep learning algorithm for simultaneous noise reduction and edge sharpening in low-dose CT images: A pilot study using lumbar spine CT. Korean J. Radiol. 22, 1850–1857 (2021).
- Hoshi, S. et al. Improvement in dacryoendoscopic visibility after image processing using comb-removal and image-sharpening algorithms. J. Clin. Med. 11 (2022).
- 17. Nakajima, K. et al. Effects of image-sharpening algorithm on surgical field visibility during 3D heads-up surgery for vitreoretinal diseases. Sci. Rep. 13, 2758 (2023).
- 18. Nakajima, K. et al. Image sharpening algorithms improve clarity of surgical field during 3D heads-up surgery. *Int. J. Retina Vitreous*. **9**, 21 (2023).
- 19. Tasaki, K., Nishimura, T., Hida, T., Maruo, K. & Oshika, T. Effects of image processing using honeycomb-removal and image-sharpening algorithms on visibility of 27-Gauge endoscopic vitrectomy. *J. Clin. Med.* 11 (2022).
- 20. Schindelin, J. et al. Fiji: An open-source platform for biological-image analysis. Nat. Methods. 9, 676-682 (2012).
- 21. Larson, M. G. Descriptive statistics and graphical displays. Circulation 114, 76-81 (2006).
- 22. Heidrich, W., Seetzen, H. & Stuerzlinger, W. High dynamic range display systems (2004).
- $23. \ \ Reinhard, E.\ High\ dynamic\ range\ imaging\ Computer\ Vision:\ A\ Reference\ Guide,\ 1-6\ (Springer,\ 2020).$

Acknowledgements

The authors thank Professor Emeritus Duco Hamasaki of the Bascom Palmer Eye Institute, University of Miami, Miami, Florida, for the discussions and thorough editing of the manuscript.

Author contributions

J.T., H.O., T.Y.: have contributed to the analysis and acquisition of data, and drafting the manuscript.; J.T., T.K.: have contributed with conception and design, analysis and interruption of data, and drafting the manuscript. M.I.: hase contributed to the conception, design, and critically reviewing the manuscript. The corresponding author (MI) had full access to all the data in the study and takes responsibility for the integrity of the data and the accuracy of the data analysis.

Funding

None.

Declarations

Competing interests

The authors declare no competing interests.

Institutional review board statement

The Institutional Review Committee of the Kyorin University School of Medicine approved the study protocol (2023-2261). This study was conducted in accordance with the Declaration of Helsinki.

Informed consent

Informed consent for data acquisition was obtained from all subjects involved in the study.

Additional information

Correspondence and requests for materials should be addressed to M.I.

Reprints and permissions information is available at www.nature.com/reprints.

Publisher's note Springer Nature remains neutral with regard to jurisdictional claims in published maps and institutional affiliations.

Open Access This article is licensed under a Creative Commons Attribution-NonCommercial-NoDerivatives 4.0 International License, which permits any non-commercial use, sharing, distribution and reproduction in any medium or format, as long as you give appropriate credit to the original author(s) and the source, provide a link to the Creative Commons licence, and indicate if you modified the licensed material. You do not have permission under this licence to share adapted material derived from this article or parts of it. The images or other third party material in this article are included in the article's Creative Commons licence, unless indicated otherwise in a credit line to the material. If material is not included in the article's Creative Commons licence and your intended use is not permitted by statutory regulation or exceeds the permitted use, you will need to obtain permission directly from the copyright holder. To view a copy of this licence, visit http://creativecommons.org/licenses/by-nc-nd/4.0/.

© The Author(s) 2025